

Calculation of radiation shielding in a SPECT-CT scanner prototype using Monte Carlo code systems

– Student Report –

submitted by

Mohga Mohamed Massoud

March 2021

Supervisor

Dr. Antonio Leyva Fabelo

JINR INTEREST PROGRAM 2021

Abstract

Nowadays it is estimated that 50% of the population exposure to radiation comes from medical sources. That's why the minimization of the received dose by both the patients and the operators of the different technologies that use radioactive sources has become a world-wide concern.

On this basis, the objective of our work was to study the effect of different experimental and geometric conditions on the dose rate in a preclinical SPECT-CT scanner prototype. A Monte Carlo-based code system (MCNPX) was used to simulate a basic experimental setup of SPECT-CT and investigate the influence on the dose rate of: different isotopic sources typical of the SPECT technique, radiation from an X-ray tube with W anode typical of CT technique, and different thicknesses of lead shielding. The results of the dose rate distribution allowed for each experimental condition to determine the safe limit distance for occupationally exposed personnel. In the text the results obtained are presented graphically and analyzed.

Acknowledgments

I would like to express my sincerest gratitude to my supervisor Dr. Antonio Leyva Fabelo for his thoughtful guidance and understanding mentoring. Not only that I learned much academically from him, improved and acquired new skills, but also it was a valuable lesson on how one can be so dedicated to his work, committed and passionate about his teaching mission. Thank you for being such a great mentor!

I would also like to thank the JINR committee for their online program and for providing me such a great opportunity!

A special thanks to my colleague Ahmed Ashref who provided an immense amount of help through the code debugging process!

Contents

1	Introduction	1
1.1	SPECT-CT	1
1.2	Understanding the radiation	2
1.3	Radiation interaction with mater	3
1.3.1	Types of interactions	3
1.3.2	What shall we consider in shielding?	4
1.4	Monte Carlo method and MCNPx code	5
2	Our model	5
2.1	The SPECT configuration	5
2.2	The shielded SPECT configuration	6
2.3	The CT configuration	6
2.4	The shielded CT configuration	7
3	Methodology and the MCNPX input file	8
4	Results	9
4.1	SPECT, ^{99m}Tc source	9
4.2	SPECT, ^{131}I source	10
4.3	CT- X-rays	11
5	Discussion	12
6	Notes on shielding	13
7	Conclusion	14

1 Introduction

1.1 SPECT-CT

Computed tomography (CT) scanning is a diagnostic imaging procedure that uses X-rays to build cross-sectional images of the body. CT is based on the fundamental principle that the density of the tissue passed by the x-ray beam can be measured from the calculation of the attenuation coefficient of the x-ray beams in the volume of the object of study. Following the measurements of the attenuation coefficients, Cross-sections are reconstructed.

The detectors of the CT scanner measure the transmission of the X-ray beam through a full scan of the body. The image of that section is taken from different angles, and this allows to retrieve the information on the depth (in the third dimension).

The CT scanner is made up of three primary systems, including the gantry, the computer, and the operating console. Each of these is composed of various sub-components. The gantry assembly is the largest of these systems. It is made up of all the equipment related to the patient, including the patient support, the positioning couch, the mechanical supports, and the scanner housing. It also contains the heart of the CAT scanner, the X-ray tube, as well as detectors that generate and detect X- rays.

Single photon emission computed tomography (SPECT) is a three-dimensional imaging technique combining the information gained from scintigraphy with that of computed tomography(CT). The main aim is the detection of the energetic photons emitted by minute amounts of radiotracers introduced into the subject of study.

The combining of the scintigraphy and the CT allows the distribution of the radionuclide to be displayed in a three-dimensional manner.

SPECT machines combine an array of gamma cameras (ranging from one to four cameras) which rotate around the patient on a gantry, providing spatial information on the distribution of the radionuclide within tissues. The projection data obtained from the cameras are then reconstructed into three-dimensional images usually in axial slices.

Most of the SPECT imaging is performed employing ^{99m}Tc (half-life of 6 hours), which is a decay product of ^{99}Mo .

The γ -ray energies, of course, differ depending on the radionuclide used and the same radionuclide may emit photons with different energies. This allows simultaneous imaging of multiple radionuclides.

SPECT may be also combined with a separate CT machine in a form of hybrid imaging; **single photon emission computed tomography-computerized tomography (SPECT-CT)** mainly for the purposes of attenuation correction and anatomical localization.

1.2 Understanding the radiation

Normally, the literature refers to the radiation emitted by nuclei as γ -rays and radiation originating in transitions of atomic electrons as **X-rays**. However, from a shielding point of view, they can be both treated as one, as shown in Figure 1, there is no fundamental difference between the two radiations for they are both electromagnetic radiation.

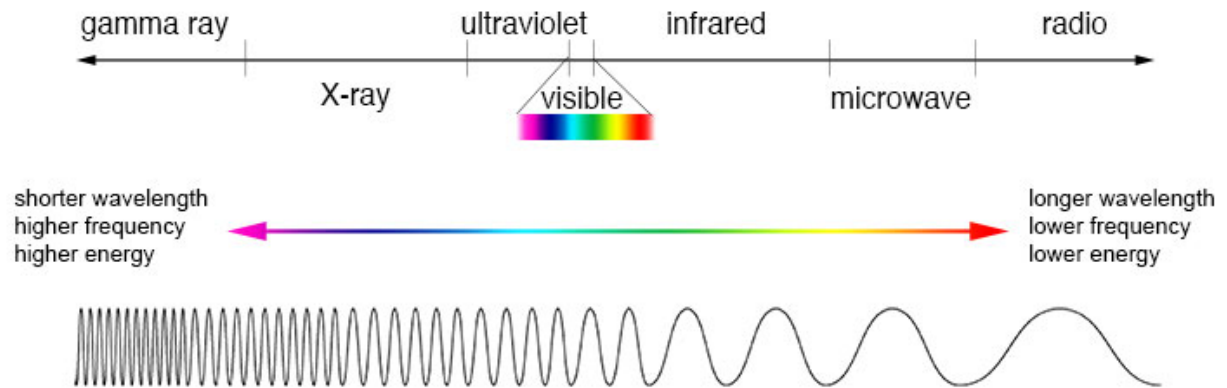


Figure 1: The electromagnetic spectrum.

When the X-ray is emitted, the X-ray spectrum has two types: Characteristic X-rays and Continuous X-rays which often called Bremsstrahlung.

Characteristic X-rays, which are shown as sharp peaks, are emitted from heavy elements when their electrons make transitions between the lower atomic energy levels which occur when vacancies are produced in the $n=1$ or K-shell of the atom and electrons drop down from above to fill the gap. The following excitation and de-excitation interactions produce the Characteristic X-rays, which are specific for Target material. Their energy doesn't depend on the operating voltage of the tube, but rather on the energy levels of the target atom.

Bremsstrahlung (which means: Brake Radiation), is a specific name for X-ray emission during electron deceleration by Coulomb forces. They don't depend on Target material, but rather on the operating Voltage of the tube and Their maximum energy is equal to the high Voltage of the Tube (in eV units). however, the probability of bremsstrahlung emission is proportional to the value of Z^2 and is thus higher for higher atomic number materials such as tungsten ($Z = 74$).

The range of photon energies emitted by the system can be adjusted by changing the applied voltage and installing filters of varying thicknesses. Filters are installed in the path of the X-ray beam to remove "soft" (non-penetrating) radiation.

X-rays are not completely absorbed inside the patient, otherwise, no image would be produced on the film. X-rays that are not absorbed, or that miss the patient, will be reflected several times by room contents until they reach the detector and referred to as "secondary beam". The primary beam, which refers to the X-ray beam prior to any interaction, is the most hazardous with a very high exposure rate. Figure 2 illustrates the X-ray beam radiation path until it reaches the detector.

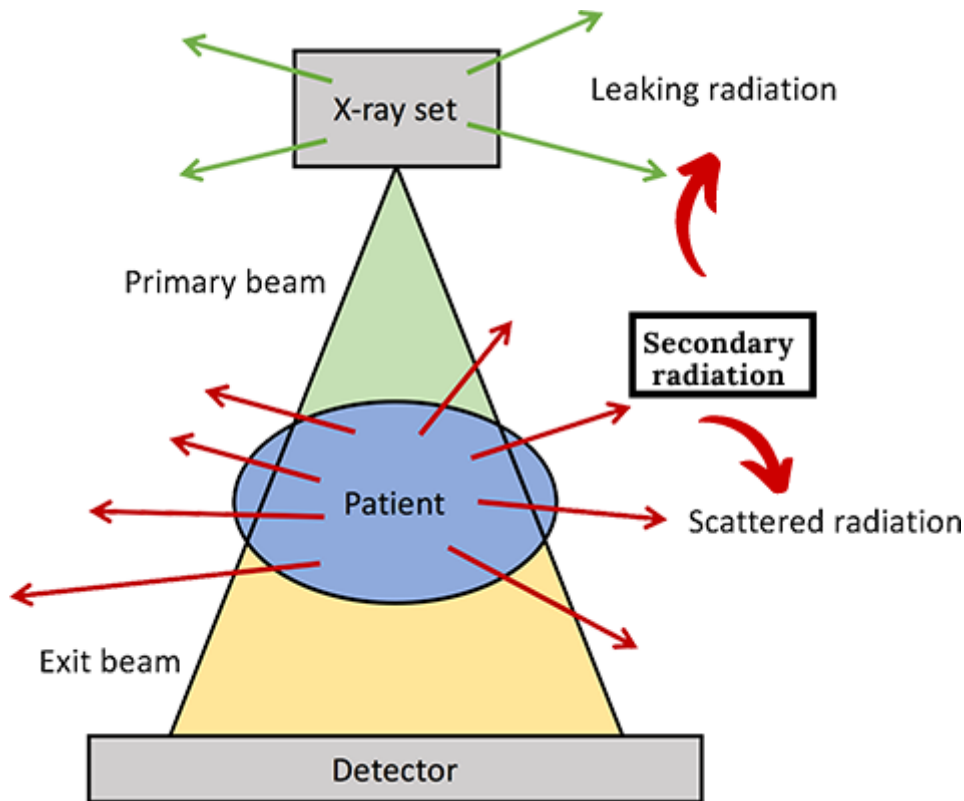


Figure 2: X-rays primary beam and secondary beam.

1.3 Radiation interaction with matter

1.3.1 Types of interactions

Photons, whether it's gamma or X-rays, interact with matter in several ways. However, only four processes are taken into account in radiation protection problems. These are Rayleigh (coherent) Scattering, the photoelectric effect, pair production and Compton effect, each of which can be represented by its own attenuation coefficient, which depends on the incident photon energy and the atomic number of the absorber material.

Rayleigh (coherent) Scattering: an electromagnetic wave passes near an electron and makes it oscillate. The oscillating electron re-radiates energy at the same frequency as the incident electromagnetic wave. In this way, there is only a photon scattering effect

for small angles. It is probable at low energy photons and for materials with high atomic numbers.

Photoelectric effect: is a phenomenon in which a photon interacts with an atom and ejects an orbiting electron resulting in the complete absorption of the photon's energy by the atom and transferring the energy to the electron. After the electron had been ejected from the atom, a hole is created in this orbital; with this, the atom is in an excited state. The hole can be filled by another electron from the external orbital, *emitting radiation known as X-ray*.

Compton (incoherent) Scattering: In this process, the photon imparts some of its energy to an electron (typically loosely bound in the outer shell) and deviates from its original direction. In this case, the photon does not disappear completely.

Pair production: a phenomenon where a photon interacts with a nucleus, completely disappears and results in creating an electron-positron pair.

The strength of these interactions depends on the energy of the X-rays and the elemental composition of the material.

1.3.2 What shall we consider in shielding?

Rayleigh scattering has a very low probability of occurrence at higher photon energy levels and low Z materials encountered in emission tomography. As for the pair production, in diagnostic nuclear medicine photon energies never reach the minimum energy required (1022 keV) for pair production.

With very low photon energies such as the soft X-ray regime and the lower hard X-ray energies, the photoelectric effect is dominant. As seen in Figure 3, the Compton effect becomes dominant from 0.1 to 0.15 MeV and onwards. For example, Compton interactions in water form over 97.4% of the total attenuation coefficients at 140 keV (0.14 MeV).

From a practical standpoint, *the Compton effect causes our most concerns in the shielding of γ -rays or X-rays*. This is because the photon does not disappear in the interaction as it does in the photoelectric effect and in pair production. The Compton-scattered photon is free to interact again in another part of the system.

Although it is true that X-rays and Auger electrons are emitted following the photoelectric effect and that annihilation radiation accompanies pair production, these radiations are always much less energetic than the initial photon and do not tend to propagate in the matter to the same extent as Compton-scattered photons, besides, that their interaction probability in our area of interest is small and Compton scattering is the most dominant interaction.

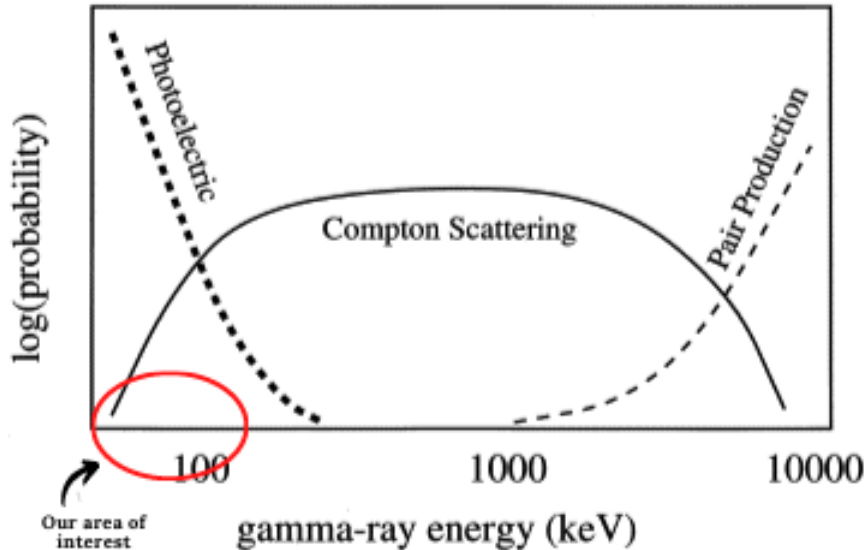


Figure 3: Radiation interaction cross sections.

1.4 Monte Carlo method and MCNPx code

The use of the Monte Carlo (MC) method in nuclear medicine calculations has increased almost exponentially in the last decades.

Monte Carlo transport codes simulate the tracks of individual particles based on detailed physics of the interaction of radiation in matter. In contrast to deterministic models, which solve the mathematical equations of radiation transport, these codes sample interactions as probability functions from cross-section data and physical concepts. For example, to estimate the absorbed dose, many particle histories are followed through the medium until the particle emerges or dies, and the losses of particles in the matter are summed.

MCNPX, which stands for Monte Carlo N-Particle eXtended, developed and maintained by Los Alamos National Laboratory, is a general-purpose Monte Carlo radiation transport code for modeling the interaction of radiation with matter. Theoretically, there is no difference between types of radiation considered. Calculation of gamma and neutron transport by Monte Carlo differs basically by handling cross sections data.

2 Our model

2.1 The SPECT configuration

Placing a mouse phantom made of A-150 tissue equivalent plastic (A-150TEP) with an isotropic point source placed at the center of the phantom. Two different sources were

considered in 2 separate cases: ^{99m}Tc source with energy = 140.5 keV and activity = 10 MBq, and ^{131}I source with energy = 364 keV and activity = 10 MBq

2.2 The shielded SPECT configuration

As illustrated in Figure 4, in front of the mouse phantom, a bed of Polypropylene with a thickness of 0.3 cm placed at 2.5 cm from the source followed by a gantry of Duralumin with a thickness of 1 cm placed at 22 cm from the source, following them, a wall of lead placed at 35 cm from the source.

The code was run for 3 different thicknesses for the lead shield: 0.5 cm, 1 cm, 1.5 cm as 3 different cases in addition to the unshielded configuration case.

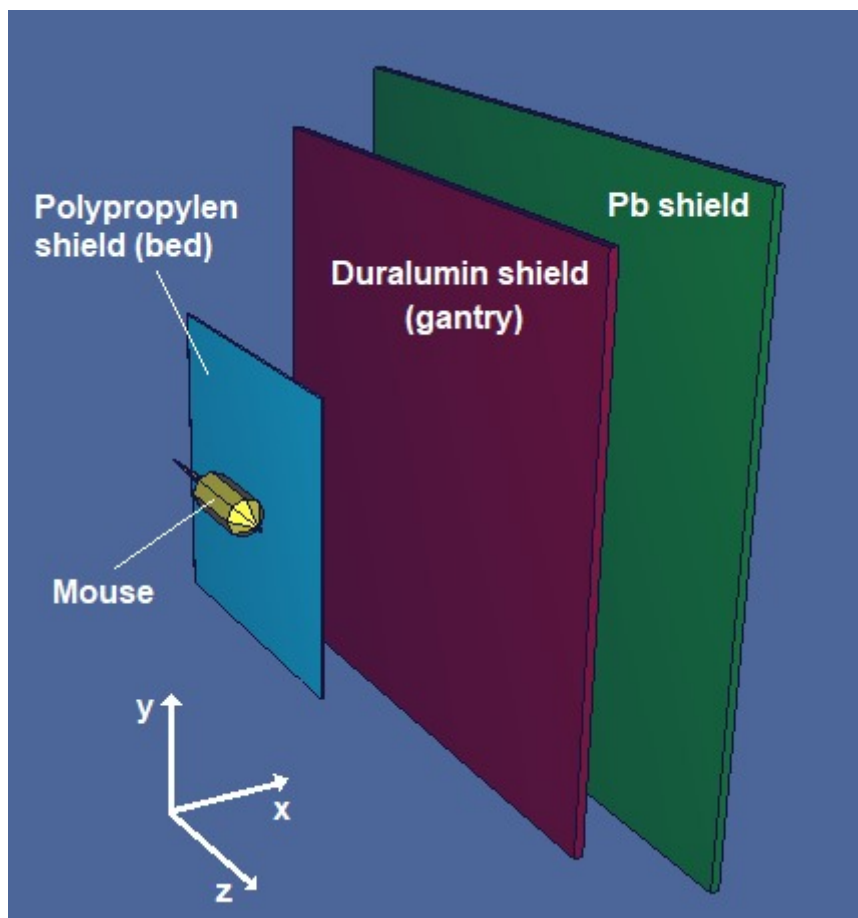


Figure 4: the shielded configuration in SPECT.

2.3 The CT configuration

The tungsten- anode X-ray tube was approximated to a point source, 1mm in front of the imaginary tungsten anode (and this represents the center of the beam in the code). The beam direction is in the direction of the phantom with a 20° angle with respect to

the x-axis.

The tungsten emission spectrum was calculated using interpolating polynomials (TAS-MIP) for potential equals to 120 keV with no filtration. Figure 5 illustrates the obtained spectrum.

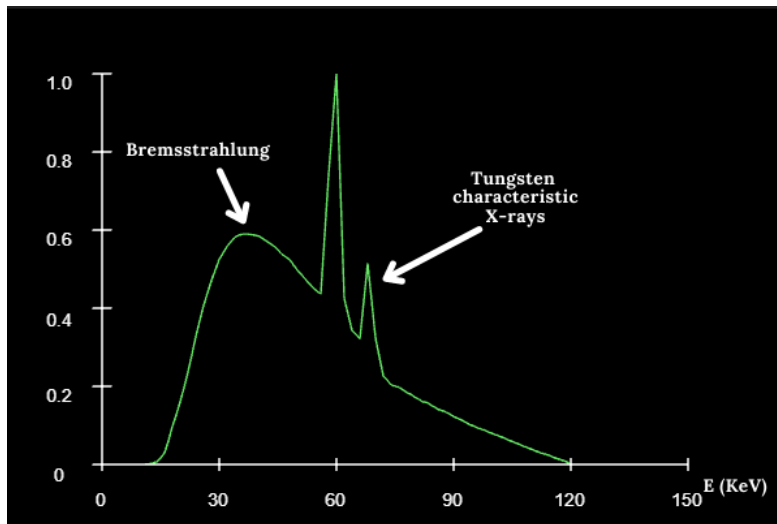


Figure 5: 120 keV X-ray spectrum for tungsten anode with no filtration.

2.4 The shielded CT configuration

As shown in Figure 6, exactly like the shielded SPECT configuration, a bed of Polypropylene with thickness 0.3 cm placed at 2.5 cm from the origin point (15.6 cm from the source) and a gantry of Duralumin placed at 35.6 cm from the source are placed in front of the mouse phantom following them, a wall of lead placed at 48.6 cm from the source.

The code was run for 3 different thicknesses for the lead shield: 0.5 cm, 1 cm, 1.5 cm as 3 different cases in addition to the unshielded configuration case.

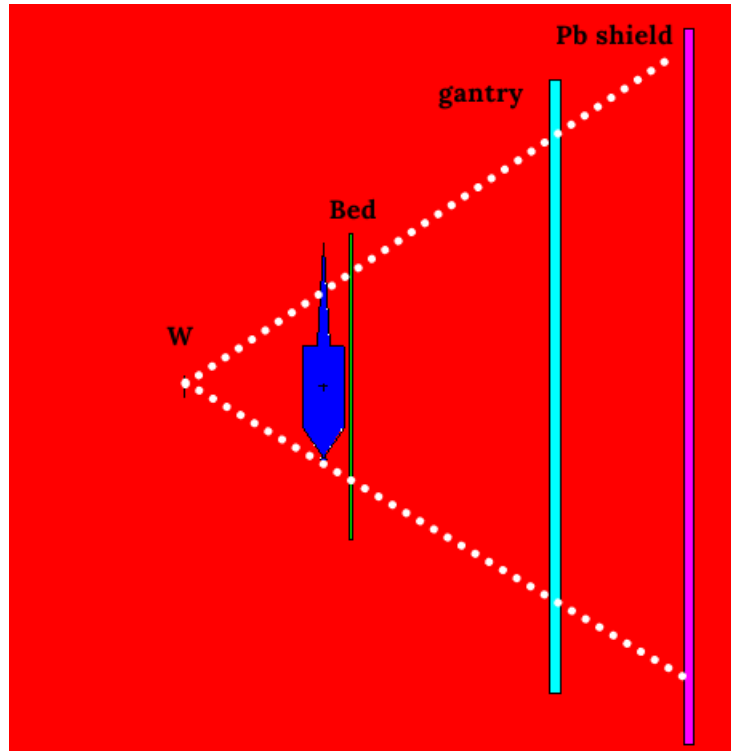


Figure 6: The shielded CT configuration.

3 Methodology and the MCNPX input file

With this configuration set, our aim is to know how much radiation is at point x, which we can call the flux or the fluence (the fluence is the time-integrated flux).

The fluence units are then converted to dose units and a distribution of the dose rate vs the distance is made, through which we can define the safe distance.

The input file:

The MCNPX input file consists of 3 main parts: cell cards, surface cards, and data cards. Both the cell and surface cards are used to describe the geometry while the data cards are used to define or describe anything other than that.

After defining the geometry, the source is defined using the source cards, with no doubt there's a great difference between the two sources in the SPECT and CT cases because of their different spectrum.

First, the SPECT case: the source is defined as an isotropic point source emitting monoenergetic photons using the SDEF card. Following that, we place point detectors at different distances on the x-axis using the tally card (F5). We use 20 tallies for 20 different positions and obtain the fluence at every tally.

A conversion from the fluence units (particle/ unit area(cm²)) to dose rate units ($\mu\text{Sv/h}$) shall be made: First, using the data from (ICRP-74, 2010), table A.1, ISO data, we

convert from particle / cm² to pSv this is done using DE and DF cards.

Second, we multiply by 3.6×10^4 using the FM card, to convert to $\mu\text{Sv/h}$. The code was run for 1×10^7 histories to obtain good results.

Analyse the output data and obtain the dose rate distribution with the distance. Now we can determine the safe distance according to the safe dose recommended, $2.3 \mu\text{Sv/h}$ as defined by ICRP-74, 2010

Repeat the same process but with the shield placed, varying the thickness of the shield with the 3 thicknesses: 0.5 cm, 1 cm, 1.5 cm to study the effect on the dose rate.

exactly the same was done in the case of the iodine-131 source for the SPECT configuration.

As for **the CT configuration**, the X-ray spectrum is different and the beam is not monoenergetic such as the γ -rays in the SPECT configuration, the X-ray tube is simplified as a point source using the SI1, SP1 and SB1 cards. Following that, just exactly like the SPECT configuration, we place point detectors at different distances on the x-axis using the tally card (F5). We use 20 tallies for 20 different positions and obtain the fluence at every tally.

A conversion from the fluence units (particle/ unit area(cm²)) to dose rate units ($\mu\text{Sv/h}$) shall be made: First, using the data from (ICRP-74,2010), table A.1, ISO data, we convert from particle / cm² to pSv , which is done using DE and DF cards.

Second, since the X-ray tube is operating at 120 keV and 350 μA , and we can say that $350 \mu\text{A} = 7.862 \times 10^{18} \text{ e}^-/\text{h}$. knowing that the efficiency of the X-ray tube is only 1% and the rest is lost in heating, we can say that the amount of photons emitted by the source is 7.862×10^{16} photons/h. Finally, multiplying by 1×10^{-6} to convert from pSv/h to $\mu\text{Sv/h}$ This is done using the FM card = 7.862×10^{10} in the input file.

4 Results

4.1 SPECT, ^{99m}Tc source

For the ^{99m}Tc source in the SPECT configuration, as shown in Figure 7, it was found that the safe distance is 23.7 cm without any shield, compared when using a 0.5 cm sheet of Pb the safe distance dropped to 21.3 cm. The lead shield insertion has decreased the

dose rate by 99.8 %.

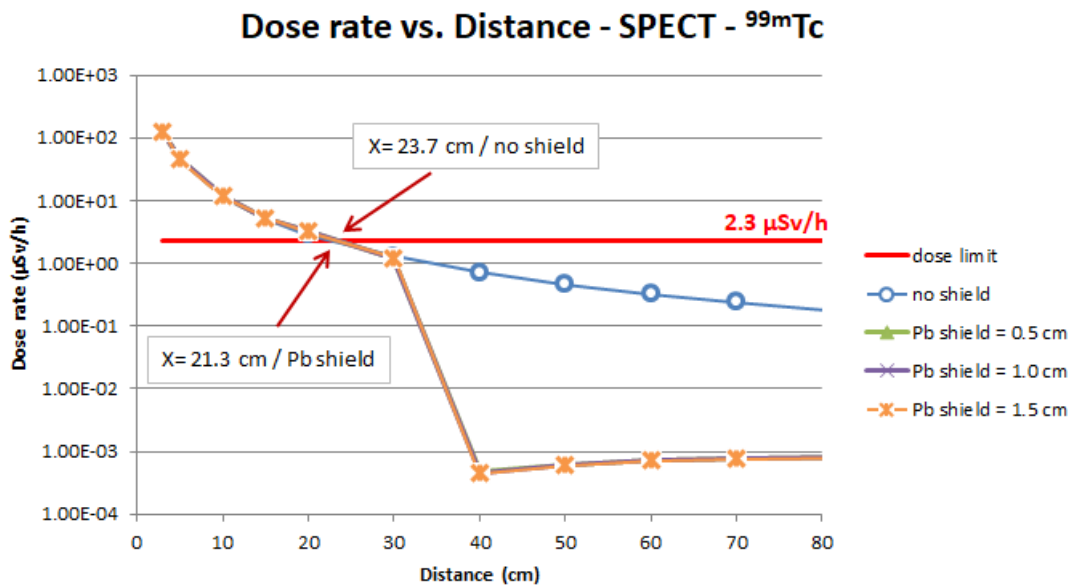
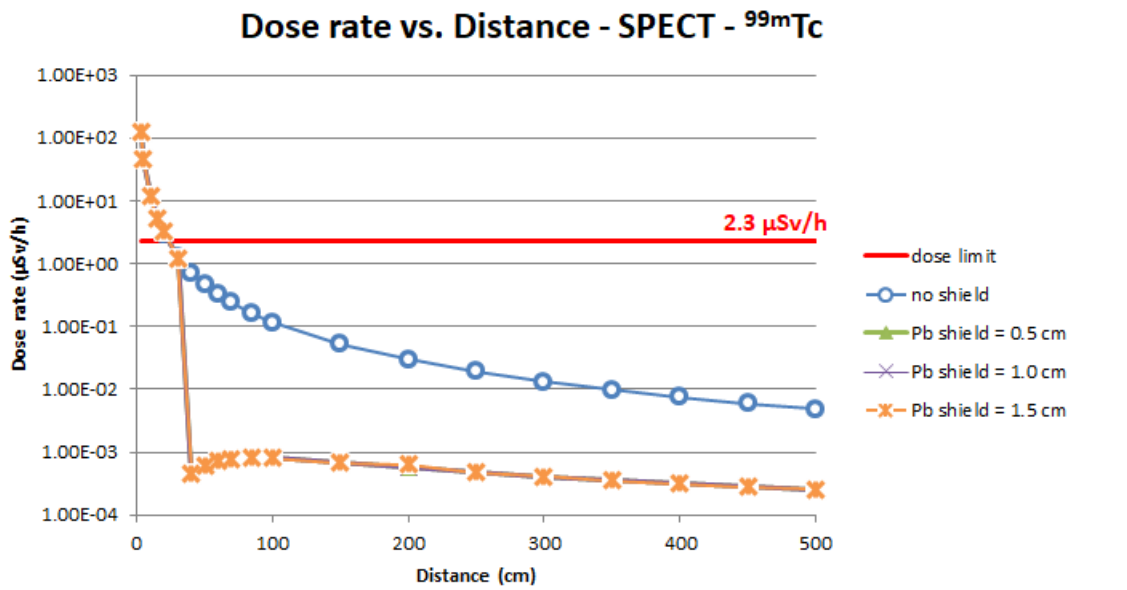


Figure 7: SPECT, ^{99m}Tc source.

4.2 SPECT, ^{131}I source

For the ^{131}I source in the SPECT configuration, as shown in Figure 8, it was found that the safe distance is 37.9 cm compared when using a 0.5 cm sheet of Pb the safe distance dropped to 33.3 cm using 1 cm of Pb, the safe distance = 33.0 cm, compared when using 1.5 cm of Pb, the safe distance = 32.9 cm.

The lead shield insertion has decreased the dose rate by 80.7 % in the case of 0.5 cm sheet, 95.5 % in the case of 1 cm sheet, 98.7 % in the case of 1.5 cm sheet.

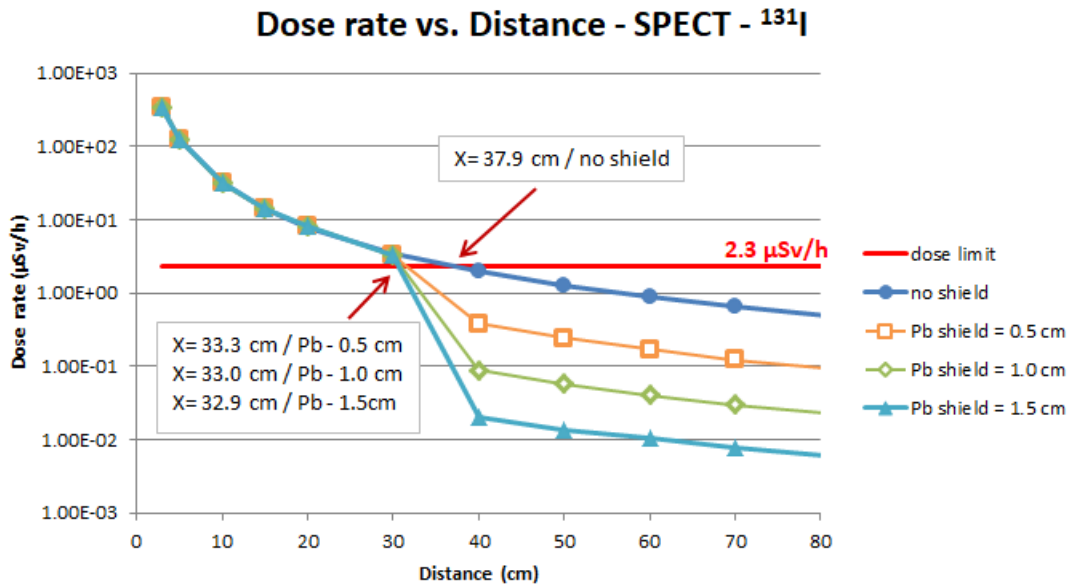
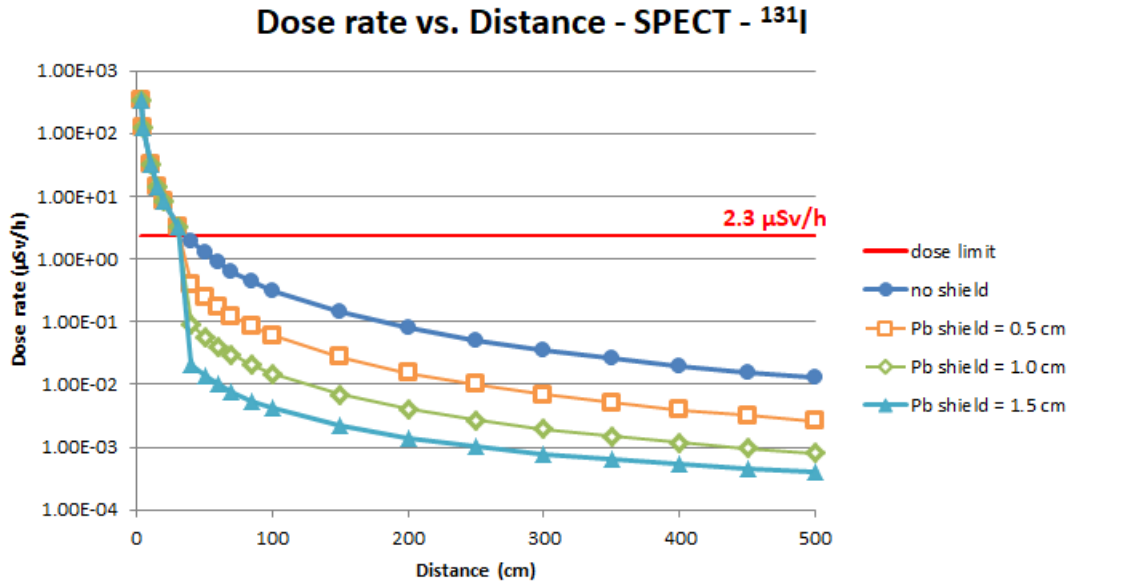


Figure 8: SPECT, ^{131}I source.

4.3 CT- X-rays

For the X-rays in the CT configuration, as shown in Figure 9, it was found that the safe distance is 9896.4 cm without shielding, comparing when using 0.5 cm sheet of Pb the safe distance dropped to 435.7 cm. The lead shield insertion has decreased the dose rate by 99.975 %

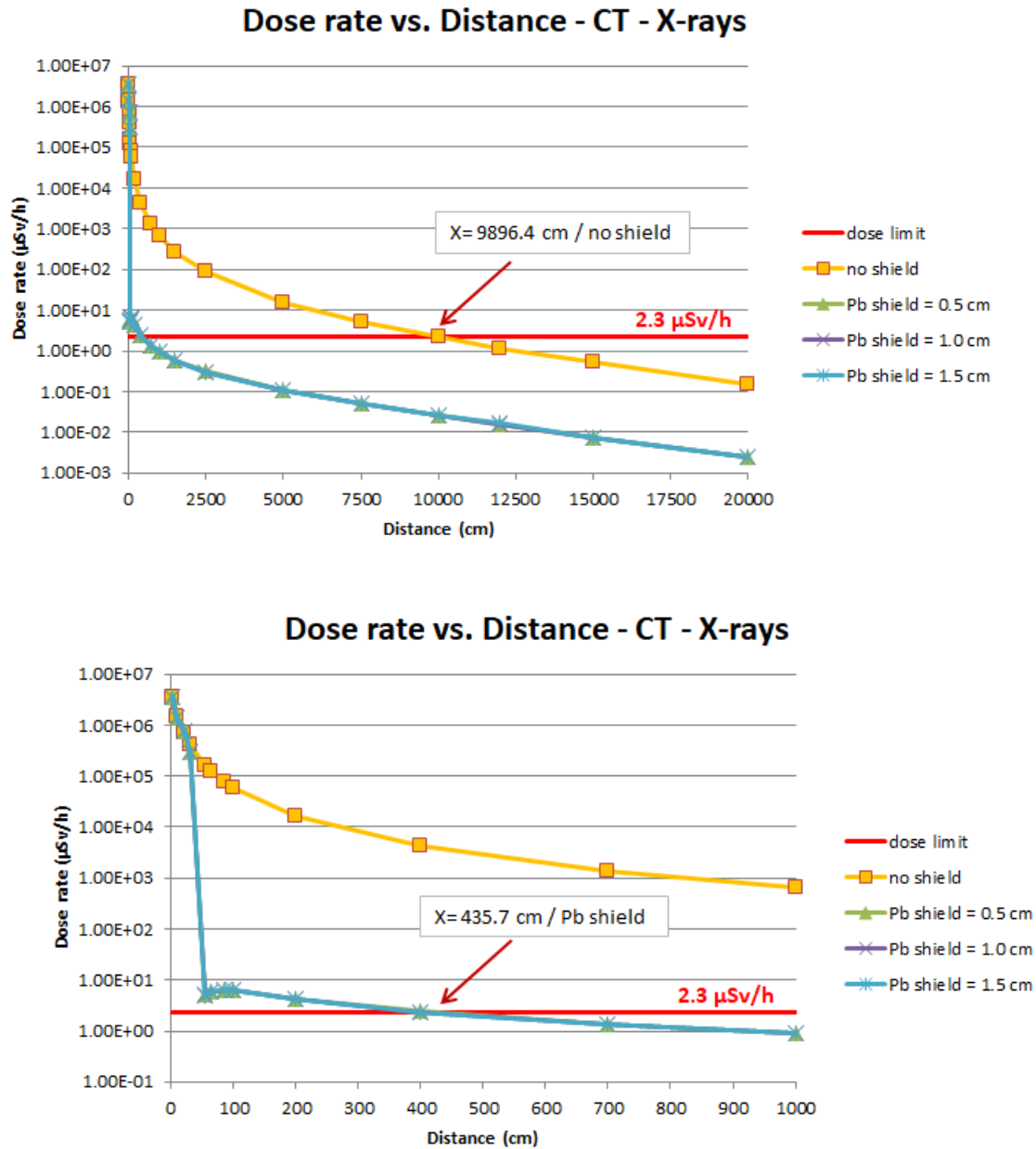


Figure 9: CT - X-rays

5 Discussion

- We notice -in all the graphs- the sudden drop of the dose rate at $x = 35 \text{ cm}$, which is the lead shield insertion point.
- **Note that** the unshielded configuration didn't contain the Polypropylene and the Duralumin shield, however, we can see that in the region before the lead insertion point, with only the Polypropylene and the Duralumin inserted, that they have very little negligible, if any, effect on the dose rate whether inserted or not.

- The reason for that is the low atomic number for the 2 materials, as the Polypropylene is mainly hydrogen and carbon and the Duralumin is 95% Aluminum ($Z = 13$), comparing to the lead ($Z = 82$) the mass attenuation coefficient for lead is nearly 14 times larger than that of the Aluminum at $E = 150$ keV.
- However the Polypropylene shield and the Duralumin shield are ineffective on their own, when followed by high Z material such as lead the shielding performance would be very different
- This is because, in Polypropylene and Duralumin, the low-energy radiation propagates with little photoelectric absorption, however, the photoelectric absorption is important in lead at low energies, owing to its high Z , and a buildup of low-energy radiation is not possible. So when the low Z material is placed before the lead, the buildup radiation from the low Z material is absorbed as it passes through the lead, and the overall buildup through the shield is small.
- ***However, if the lead is placed first***, the subsequent buildup of radiation in the polypropylene and the Duralumin layer will reach the observer and the overall buildup is larger.
- In SPECT- ^{99m}Tc case, we can notice that the change in the different thicknesses of the lead shield from 0.5 to 1 to 1.5 cm yields a very slight and nearly unnoticeable change in the dose rate. In contrast to the SPECT- ^{131}I case that's due to the difference in the source energy, the iodine source has 2.5 times more energy than the technetium source.
- X-ray radiation needs much stronger shielding than γ -rays.

6 Notes on shielding

- The basic shielding requirements for radiation protection depend on several factors: The type of radiation encountered, length of exposure, and distance from the source of radiation.
- The longer one must be exposed directly or indirectly to radiation, the greater the level of shielding required. *For medical and dental patients*, the length of direct exposure to X-rays is very brief
- The weight, space, cost, and attenuation or absorption capabilities of the material used for radiological protection are key points to choose the right material for your configuration.

- The toxicity of the lead is now a concern and more research is conducted to have a "lead free" shielding for X-ray. Bismuth and its compounds, especially Bismuth Fluoride (BiF_3) for its high mass attenuation coefficient, seems promising, however, more search is still needed.

7 Conclusion

The use of 0.3 cm-Polypropylene, 1 cm-Duralumin and varying thicknesses of Lead (from 0.5 cm, 1 cm to 1.5 cm) as a shield for the proposed SPECT-CT configuration proved to have a noticeable effect on the dose rate.

The proposed shield decreases the dose rate by 98.3% in SPECT- ^{99m}Tc and 99.9% in the CT configuration leading to a minimization of the required safe distance, from 23.7 cm to 21.3 cm in the case of SPECT- ^{99m}Tc and from 9896 cm to 436 cm in the case of the CT configuration.

References

- [1] I. A. E. AGENCY. *Diagnostic radiology physics: a handbook for teachers and students*. International atomic energy agency, 2013.
- [2] J. M. Boone and J. A. Seibert. An accurate method for computer-generating tungsten anode x-ray spectra from 30 to 140 kv. *Medical physics*, 24(11):1661–1670, 1997.
- [3] R. G. Jaeger, E. Blizard, M. Grotenhuis, A. Hönig, T. A. Jaeger, and H. Eisenlohr. *Engineering Compendium on Radiation Shielding. Volume 1. Shielding Fundamentals and Methods*. Springer, 1968.
- [4] J. R. Lamarsh and A. J. Baratta. *Introduction to nuclear engineering*, volume 3. Prentice hall Upper Saddle River, NJ, 2001.
- [5] R. J. McConn, C. J. Gesh, R. T. Pagh, R. A. Rucker, and R. Williams III. Compendium of material composition data for radiation transport modeling. Technical report, Pacific Northwest National Lab.(PNNL), Richland, WA (United States), 2011.
- [6] D. B. Pelowitz, J. W. Durkee, J. S. Elson, M. L. Fensin, J. S. Hendricks, M. R. James, R. C. Johns, F. W. Mc Kinney, S. G. Mashnik, L. S. Waters, et al. Mcnpx 2.7 e extensions. Technical report, Los Alamos National Lab.(LANL), Los Alamos, NM (United States), 2011.
- [7] N. Petoussi-Henss, W. Bolch, K. Eckerman, A. Endo, N. Hertel, J. Hunt, M. Pelliccioni, H. Schlattl, and M. Zankl. Conversion coefficients for radiological protection quantities for external radiation exposures. *Annals of the ICRP*, 40(2-5):1–257, 2010.
- [8] G. Saldaña, U. Reyes, H. Salazar, M. Oscar, E. Moreno, and R. Conde. *High Density Devices Applied to a Gamma-Camera Implementation*. March 2012.